Journal of Applied Polymer Science

Plasticizer Migration in Bloodmeal-Based Thermoplastics

James Michael Bier, Casparus Johannes Reinhard Verbeek, Mark Christopher Lay
School of Engineering, University of Waikato, Private Bag 3105, Hamilton 3240, New Zealand
Correspondence to: J. M. Bier (E-mail: jmb101@waikato.ac.nz)

ABSTRACT: Tri-ethylene glycol (TEG) is an effective plasticizer for many protein-based thermoplastics because of its low volatility, however, partial miscibility with the protein matrix may still lead to some phase separation. Spatial variation of TEG concentration in bloodmeal-based thermoplastics as a result of processing was investigated using synchrotron-based FT-IR micro-spectroscopy. Although TEG forms strong hydrogen bonding with proteins, for the protein to fold into β-sheets bound plasticizer must be released. TEG can then migrate, pooling into localized areas, rich in plasticizer. Further heating causes further migration towards the edge of plasticized bloodmeal particles where the TEG may evaporate. Thermo-gravimetric analysis confirmed that loss of TEG by evaporation may occur at 120°C, given enough time for diffusion. Efficient mixing combined with a short residence time at elevated temperature mean significant plasticizer loss is unlikely during processing. However, it does limit long-term use at elevated temperatures. © 2013 Wiley Periodicals, Inc. J. Appl. Polym. Sci. **2014**, *131*, 39969.

KEYWORDS: biopolymers and renewable polymers; plasticizer; proteins; spectroscopy; thermogravimetric analysis

Received 31 May 2013; accepted 12 September 2013
DOI: 10.1002/app.39969

INTRODUCTION

Bloodmeal is a by-product of the meat processing industry, which can be extruded into a bio-based thermoplastic by mixing with a reducing agent, protein denaturant, surfactant, and plasticizer.[1,2] The resulting material is known as Novatein™ thermoplastic protein (NTP). Extrusion of proteins involves applying heat and shear to produce a homogenous melt. This involves denaturing, disassociation, unravelling, and re-alignment of protein chains.[3] After compounding, NTP can be extruded or injection moulded using conventional polymer processing equipment.

Water is a common plasticizer for protein-based thermoplastics, but evaporation after processing can result in a brittle material.[4] For this reason, less volatile plasticizers are often used instead of or in conjunction with water. Tri-ethylene glycol (TEG) has been shown to be an effective plasticizer in bloodmeal-based thermoplastics; remaining in injection-moulded test pieces during conditioning, resulting in a tougher and more ductile plastic material.[5]

Urea is included in NTP to assist in disrupting protein–protein interactions during processing. Urea also has a plasticising function, and in the absence of TEG a ductile material can be produced if enough urea is included in the formulation.[4] However, urea can leach out of protein plastics forming a white residue on the plastic's surface.[3,6,7] Urea, water, and TEG all contain polar groups and hydrogen bond to protein chains. TEG also contains hydrophobic groups and therefore should show slower leaching rates compared to urea and water. A study of corn protein-based thermoplastics with a wide variety of plasticizers suggested polar plasticizers interact with easily accessible polar amino acids, but amphiphilic plasticizers could interact with more difficulty to access nonpolar zones, buried with the protein.[8]

Plasticizer migration in conventional plastics faces public scrutiny because of concerns about biological impacts, for example concerns about potential carcinogenicity and endocrine disruption effects of phthalates.[9,10] Traditional plasticizers used with synthetic polymers are not necessarily suitable for some bio-based plastics and along with water, polyols are more common.[11,12] Nevertheless, plasticizer migration is still of interest for protein-based materials, as it has potential implications for both processing and resultant material properties. If the plasticizer concentration is too high, it can exceed the compatibility limit leading to phase separation and plasticizer exclusion.[11] Phase separation into plasticizer-rich and plasticizer-poor phases has been implicated in the presence of multiple thermal transitions in soy protein-based plastics.[13] In wheat gluten composites reinforced with natural fibers, migration of plasticizer from the matrix to the fiber results in a more brittle matrix with higher glass transition temperature. This effect reduces processability at high fiber contents.[14]

The migration rate of plasticizers in proteins depends on the physicochemical properties of the plasticizer,[8] but is also influenced by other factors such as protein conformation and environmental conditions. A study of plasticized wheat gluten films suggested plasticizer migration may be reduced by a more

aggregated protein structure.[15] Certain plasticizers may have different compatibilities with different proteins. For example, polyethylene glycol was found to be compatible with wheat grain protein, but less compatible with β-lactoglobulin or soy protein isolate, as evidenced by the formation of an oily surface residue.[16] Environmental factors such as humidity may also promote migration of plasticizer from proteins.[17] For films made of sunflower protein, reasonable barrier properties for water vapor were obtained, but resistance to water was limited, in part because of migration of hydrophilic plasticizers into the water.[12] Another environmental consideration is temperature. Even with conventional plastics, materials used in high temperature environments often need frequent replacement because of becoming brittle and cracking as plasticizers evaporate or degrade over time.[9] It is therefore of interest to determine how protein/plasticizer interactions are affected during heating.

FT-IR is commonly used with protein-based plastics to estimate relative amounts of secondary structures using the amide I (1600–1700 cm^{-1}) or amide III (1180–1330 cm^{-1}) regions of the spectra. Analysis of peaks corresponding to plasticizer functional groups can yield more information about the interactions of the protein with the plasticizer. For example, FT-IR analysis revealed no covalent interactions had formed between glycerol and protein sheets prepared from soy protein isolate, as no changes were observed in the peaks characteristic of each component.[18] However, FT-IR of soy protein plastics plasticized with both glycerol and caprolactone indicated that caprolactone had been consumed in their preparation as its characteristic peaks were not observed.[19]

TEG contains both ether and alcohol functional groups and absorbance peaks corresponding to these are present in bloodmeal-based plastics containing TEG.[5] Analysis of how these peaks change relative to characteristic protein peaks across a sample should reveal how plasticizer content changes spatially as the result thermoplastic processing.

Spatially resolved secondary structure changes occurring in bloodmeal-based plastics because of processing have previously been reported.[20] β-sheets were concentrated around the perimeter of bloodmeal particles, whereas after extrusion and injection moulding, β-sheet-rich regions were distributed more evenly throughout a disordered matrix. At each processing stage, the inclusion of TEG as a plasticizer resulted in more random coils and less α-helices and β-sheets throughout the material. Because urea also has a carbonyl absorbance peak in the amide I region, analysis relied on the amide III region. Although weaker than the amide I, it is also sensitive to structural changes.

The work presented here discusses the spatial distribution of TEG and include peaks corresponding to both the alcohol and ether groups from TEG. The primary objective was to determine how these change relative to the amide III region on heating pre-extruded powder as well as after different processing steps. Results are used to explain how protein/plasticizer interactions vary spatially on a microscale and how these are influenced by heating and thermoplastic processing.

Table I. Composition, in Parts Per Hundred Bloodmeal (pph_{BM}) of the Pre-extruded Formulations

	PNTP-TEG	PNTP-V0	PNTP-U0
Bloodmeal	100	100	100
Water	40	60	40
TEG	20	0	20
Urea	10	10	0
SDS	3	3	3
SS	3	3	3

EXPERIMENTAL

Materials and Sample Preparation

Pre-extruded NTP (PNTP) was prepared as described previously[20] using agricultural grade bloodmeal (Wallace Corporation, Hamilton, New Zealand), agricultural grade urea (Ballance Agrinutrients, Kapuni, New Zealand), distilled water, TEG for synthesis (Merck), technical grade sodium dodecyl sulphate (SDS) (Merck), and technical grade sodium sulphite (SS) (Merck) (Table I).

After mixing, the product (PNTP-TEG) was equilibrated overnight below 4°C in sealed plastic bags. Additional formulations containing no TEG (PNTP-V0) and no urea (PNTP-U0) were also prepared for thermal analysis (Table I).

PNTP-TEG was extruded (ENTP), granulated and injection moulded (INTP), and conditioned (CNTP) using previously described parameters.[20] Samples from each processing step were dried over two nights in a Freezone® 2.5 Litre bench-top freeze dryer (Labconco Corporation, Kansas City) set to auto mode (Collector temperature −50°C, vacuum <11 Pa.) before transport to the Australian synchrotron.

Analysis

Synchrotron FT-IR Microscopy. FT-IR experiments were conducted on the infrared micro-spectroscopy beamline at the Australian Synchrotron, Victoria, Australia. For thermal experiments, particles of PNTP-TEG were flattened between two diamond cells then transferred to a barium fluoride slide for analysis in a Linkham FTIR 600 (Linkham Scientific Instruments) heated stage. Sections of ENTP, INTP, and CNTP 2 μm thick were cut using stainless steel blades (TBS^{TM}) on a TBS Cut 4060 RE microtome (TBS^{TM}) lit by a microlight 150 (Fibreobtic Lightguides, Australia). The microtomed ribbons were then flattened between two diamond cells, then the top cell removed for analysis. Spectra were collected using Bruker Hyperion 3000 equipped with an MCT collector and motorized XY stage and using Opus 6.5 software (Bruker Optik GmbH 2009). For each sample, video images were first captured using Opus 6.5, then grids of points to be scanned chosen. Thirty-two spectra were collected and averaged for each grid point with a resolution of 4 cm^{-1} between 3900 and 700 cm^{-1}.

Three types of experiments were performed on PNTP-TEG to determine the effect of thermal treatment on the pre-extruded material, each with freshly mounted samples:

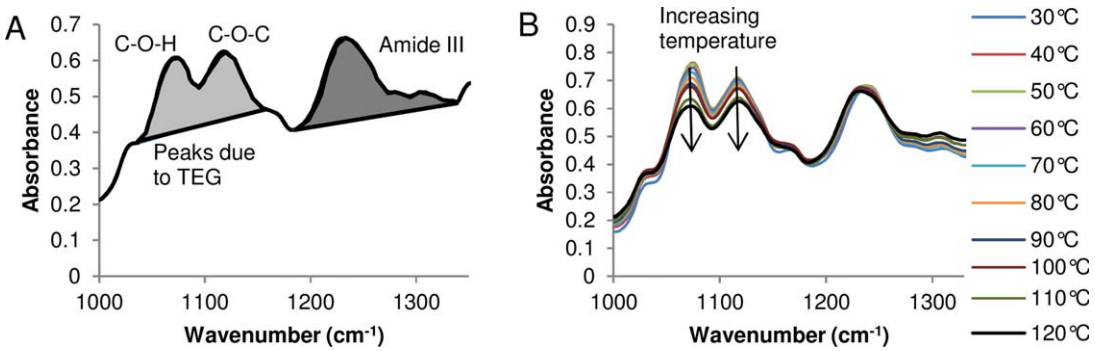

Figure 1. (A) Peaks in FT-IR spectra because of amide III region and those attributed to functional groups in TEG. (B) Changes in peak height as a function of temperature. [Color figure can be viewed in the online issue, which is available at wileyonlinelibrary.com.]

- A 50 × 50 μm spot was chosen to average out spatial variations and spectra were collected at 30-second intervals during a constant heating ramp from −120°C to 120°C at 2°C /min.
- Representative grids with a 10 × 10 μm spot size were mapped in *x–y* coordinates on four separate particles. After spectra collection for each point in the grids, the mounted samples were heated to 120°C, held isothermally for 2 min then returned to room temperature. Spectra were then collected for grids with the same *x–y* coordinates as originally scanned.
- Smaller representative grids, also with a 10 × 10 μm spot size were mapped on three separate particles at room temperature. These samples were then heated to 50°C. Grids with the same *x–y* co-ordinates were mapped again after a 10-min isothermal soak time. This process was repeated at 70°C, 90°C, 110°C, and 130°C.

Microtomed sections of processed (extruded, extruded then injection moulded, extruded then injection moulded, and conditioned) plastic were also examined for spatial distribution but not subjected to additional thermal treatments.

Data Analysis. FT-IR spectra for each point were used to prepare spatial maps of integrated peak ratios using OPUS 6.5. Opus type B integrals were calculated from 1040 to 1150 cm^{-1} (C-O-C and C-O-H functional groups in TEG) and from 1180 to 1330 cm^{-1} (amide III region of proteins), along with the ratio of the first peak over the second. These ratios were used to compare TEG distribution relative to protein in spatial maps. Using peak area ratios has the advantage of eliminating effects of variation in thickness across samples.[21] The ratio between the areas corresponding to each of the two functional groups of TEG (1040–1095 cm^{-1} for C-O-H and 1095–1150 cm^{-1} for C-O-C) was also calculated and examined. Mean, standard deviation, median, upper quartile, and lower quartiles were calculated for the mapped ratios. Data were filtered for a minimum area under the amide III region to exclude points mapped outside particles from statistical analysis.

Thermogravimetic Analysis. Thermogravimetic analysis (TGA) was performed in a Texas Instruments SDT 2960 analyzer using approximately 10 mg of sample in dry air. Freeze dried PNTP-TEG and PNTP-V0 were heated at a constant rate of 10°C/min from room temperature to 700°C. Samples of PNTP-TEG, PNTP-V0 and PNTP-U0 were also analyzed by heating at a constant rate of 10°C/min from room temperature to 120°C and holding at 120°C 3 h.

RESULTS AND DISCUSSION

Thermally Resolved FT-IR

Temperature-Resolved Changes. Bloodmeal-based thermoplastics containing 20 pph_{BM} TEG showed two similar sized peak regions between 1000 and 1350 cm^{-1} attributed to the amide III region (1180–1330 cm^{-1}) and TEG (1040–1150 cm^{-1}) [Figure 1(A)]. Two peaks were observed between 1040 to 1095 cm^{-1} and 1095 to 1150 cm^{-1}. These correspond to expected locations for primary alcohols and aliphatic ethers, respectively, both functional groups present in TEG. Neither peak was apparent in samples that did not contain TEG, therefore it is reasonable to conclude these correspond to vibrations of the C-O bond in the C-O-H and C-O-C functional groups of TEG [Figure 1(A)].

The peaks corresponding to C-O bonding in TEG significantly decreased in intensity when heated from room temperature to 120°C [Figure 1(B)]. A small change in shape was also observed in the amide III region, with a slight shifting of the convoluted peak centered around 1240 cm^{-1} to a lower wavenumber. This shape change was taken to be indicative of increasing β-sheets at the expense of random coils.[5,20]

The alcohol peak intensity (C-O-H, Figure 1) decreased more than the ether group (C-O-C), which suggests a reduction in OH groups. Looking at higher wavenumbers, where stretches of X-H bonds are found (Figure 2), there was also a change in shape and intensity over the same temperature range, with a

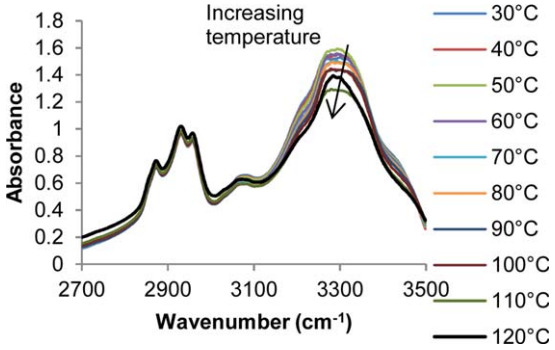

Figure 2. Change in spectral region corresponding to X-H bond vibrations. [Color figure can be viewed in the online issue, which is available at wileyonlinelibrary.com.]

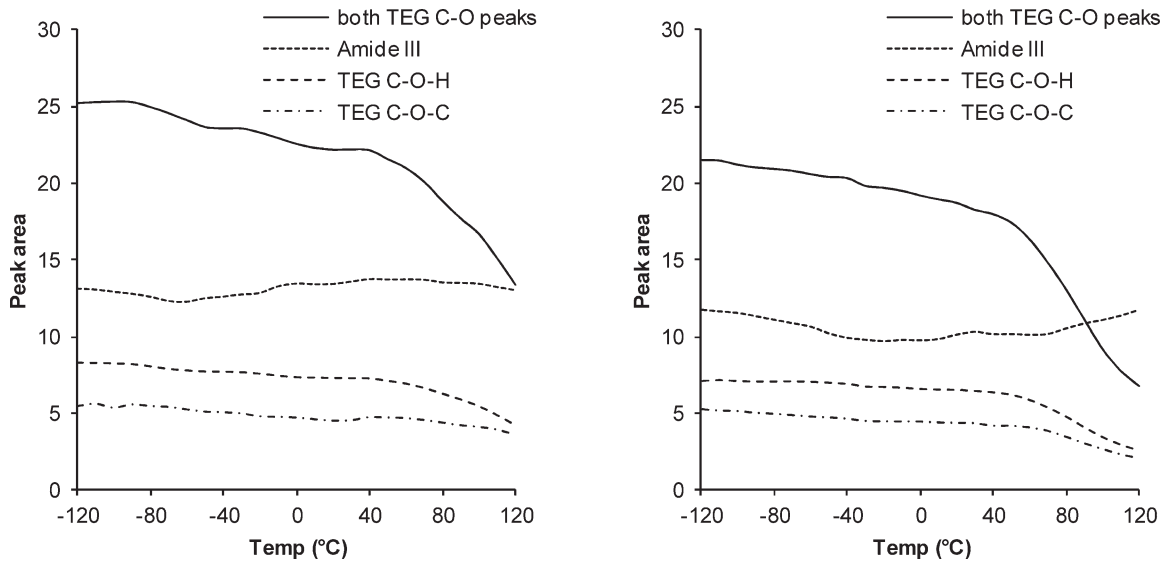

Figure 3. Integrated peaks versus temperature during heating at 2°C/min for 50 x 50 μm spots on two separate PNTP-TEG particles.

decrease and a shift from higher wave number to lower wavenumber. O-H stretching can spread throughout this region (from 3000 to 3500 cm^{-1} and beyond), but N-H stretching would typically be in the lower end of this region. This change in shape would therefore be consistent with a reduction in amount of OH groups present when the plastic is heated. C-H stretches also absorb in this region, but further interpretation from this spectral region is complicated by potential contributions from the large amount of functional groups in different environments possible in protein side groups, the protein backbone and those in TEG.

There was little discernable change in peaks at 2920 and 2850 cm^{-1} when the plastic was heated from room temperature to 120°C (Figure 2). These peaks correspond, respectively, to asymmetric and symmetric stretches in CH_2 aliphatic regions. Reduction of these peak heights is typically indicative of side chain degradation in proteins (such as keratin[22,23]). For NTP, analysis of this region is complicated by CH_2 groups in both protein side chains and in TEG.

To ensure that the trends seen were repeatable, another particle was tested in the same fashion, and peak area versus temperature was plotted for both (Figure 3). In both cases a gradual decrease in area corresponding to TEG's C-O peaks was seen during heating up to 40°C, with a sharper drop beyond this. There was some fluctuation in the size of the amide III, but little discernable trend. Within TEG's C-O peaks, the C-O-H peak showed a greater drop in area than the C-O-C peak in both cases. Although both particles show the same trends, there is some difference in the initial areas of each group, suggesting different sample thicknesses, and potentially different initial TEG concentrations between the two particles.

The decrease in functional groups would indicate either some TEG is lost during heating or that the interaction between protein chains and TEG is changing thereby masking the presence of TEG. If TEG evaporates, it would cause the material to be more brittle. It was thought that more insight could be obtained by not only examining how the peaks changed relative to each other on heating, but also if there was any spatial variation within samples.

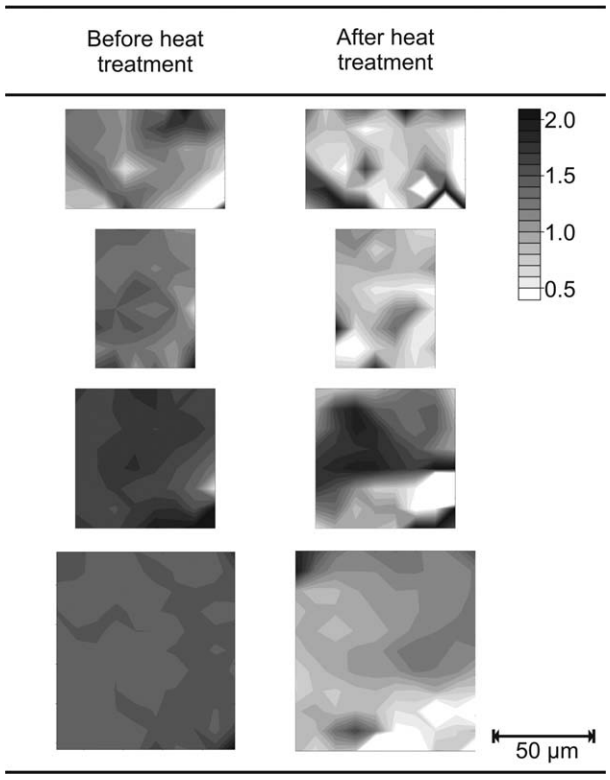

Figure 4. Spatial maps of ratio between peak integrals representing TEG (1040–1150 cm^{-1}) and the amide III region (1180–1330 cm^{-1}) as the same four grids (10 x 10 μm spot size) on four separate FD PNTP-TEG particles were scanned before and after 2-min isothermal heat treatment at 120°C. Darker shading indicates higher relative TEG content.

Table II. Summary Statistics for Grids Mapped on PNTP-TEG Particles Before and After Thermal Treatment at 120°C for 2 min

	Before heating		After heating	
	TEG/amide III	COH/COC	TEG/amide III	COH/COC
Mean	1.53	1.62	1.05	1.60
Standard deviation	0.30	0.22	0.40	0.93
Lower quartile	1.38	1.49	0.79	1.37
Median	1.62	1.54	0.98	1.46
Upper quartile	1.71	1.69	1.23	1.62

Filtered for a minimum integrated area of 5 under the amide III region and excluding negative ratios to exclude points outside particles.

Spatial Distribution Before and After a Heat Treatment. Freeze dried PNTP-TEG showed a heterogeneous distribution of TEG throughout the particles (Figure 4). There was some variation between separate particles, with some particles showing regions with up to twice the area for the peaks corresponding to TEG to that of the amide III, and some regions with only half the amide III area. For the most part, however, the approximate area ratio was 1–1.5 to 1. It is important to note that this does not imply equal or higher TEG concentration in the plastic than protein, as TEG will absorb differently to protein. The area ratio, however, will show if there is change in the relative concentration of TEG across a map, as is the case here.

After a 2-min isothermal period at 120°C (simulating the residence time of an extruder), spatial maps of the same *x–y* coordinates of the same FD-PNTP particles were noticeably different (Figure 4). The spatial maps became even more heterogeneous, with some regions darkening and others lightening when drawn on the same intensity scale. This suggests migration of TEG within the plastic as molecular mobility was increased with increasing temperature. As well as an overall decrease in the average TEG/amide III peak ratio, an increase was seen in the standard deviation and the difference between the upper and lower quartile values (Table II). The C-O-H/C-O-C peak ratio was approximately the same on average across the maps, but the standard deviation increased (Table II).

Spatial Distribution at Elevated Temperatures. Freshly mounted samples of PNTP-TEG were examined at 23°C, then the same regions remapped at progressively higher temperatures. TEG content increased towards the edge of the mapped grids, closer to the edges of particles with increasing temperature (Figure 5) and then was partially removed at higher temperatures. While short isothermal treatments led to more heterogeneous distributions, increasing homogeneity was seen after equilibrating samples for 10 min at each temperature before scanning. This was evident from a decreasing standard deviation for the average TEG/ amide III peak area ratio across the maps, along with smaller difference between the lower and upper quartiles (Table III). The C-O-H to C-O-C peak ratio also decreased. This could either mean the strength of the absorbance with concentration varied for the two different functional groups, or it could suggest some plasticizer migration or interaction between protein and TEG interfering with end groups on the TEG molecules.

It has previously been reported that bloodmeal particles are more amorphous in the center, with a higher concentration of β-sheets at the edges, and α-helices scattered throughout. After processing there is a more homogenous distribution, with an overall increase in β-sheets. Samples with 20 pph_{BM} TEG show reduced β-sheets compared with samples without TEG at each processing step.[20] Both α-helices and β-sheets are stabilized by strong hydrogen bonding interactions involving the NH and C=O groups of the polypeptide backbone. In randomly coiled structures, these groups may be hydrogen bonded to solvent or plasticizer instead of each other. The observed conformational change from random coils to β-sheets would require bound plasticizer to transition to free plasticizer as protein–protein hydrogen bonding interactions replace hydrogen bonding interactions with TEG. This free plasticizer is then free to migrate through the material. When soy protein sheets were heated, kinetic studies showed the rate of conformational change was

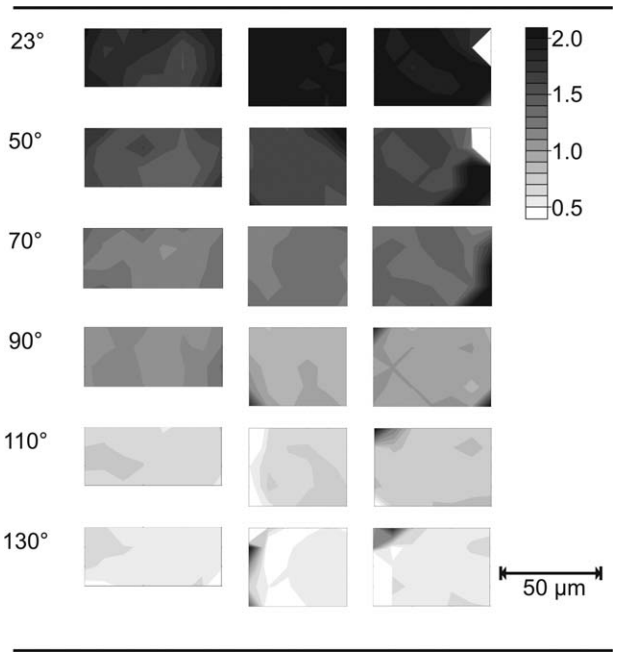

Figure 5. Spatial maps of ratio between peak integrals representing TEG (1040–1150 cm^{-1}) and the amide III region (1180–1330 cm^{-1}) as the same three grids on separate FD PNTP-TEG particles were scanned at progressively higher temperatures. Darker shading indicates higher relative TEG content.

Table III. Summary Statistics for Grids Mapped on PNTP-TEG Particles at Progressively Higher Temperature

	TEG/amide III						COH/COC					
Temperature (°C)	23	50	70	90	110	130	23	50	70	90	110	130
Mean	1.96	1.62	1.34	1.02	0.74	0.55	1.60	1.63	1.55	1.45	1.30	1.26
Standard deviation	0.15	0.12	0.09	0.06	0.08	0.06	0.10	0.11	0.11	0.11	0.17	0.16
Lower quartile	1.88	1.56	1.28	0.97	0.71	0.53	1.52	1.53	1.46	1.35	1.22	1.18
Median	2.00	1.62	1.34	1.02	0.74	0.56	1.61	1.65	1.55	1.47	1.33	1.28
Upper quartile	2.05	1.66	1.39	1.07	0.78	0.58	1.68	1.70	1.61	1.52	1.38	1.34

Filtered for a minimum integrated area of 5 under the amide III region to exclude points outside particles.

too fast to be explained by evaporation of water alone.[24] This would suggest that structural rearrangement is the driver for plasticizer migration, rather than the other way around.

Processing

The ratio of the peak area corresponding to the C-O-H group of TEG to the amide III region was previously used to get an impression of the change in TEG distribution induced by processing.[20] Considering the TEG peaks discussed in this article, similar trends were seen (Figure 5). After extrusion, there was a more homogeneous distribution than in the pre-extruded powders, but still some localized phase separation. Injection moulding smoothed out local variations, but when the full C-O-X region was used to evaluate TEG relative to protein, it could be seen that some larger range phase separation was occurring, giving a broader statistical distribution (Table IV). After conditioning, more localized concentrated spots appeared again (Figure 6).

Comparing the TEG/amide III ratio spatial distribution for the processed plastics with the C-O-H/C-O-C peak ratios provides an interesting contrast to the thermal experiments. The C-O-H peak decreased relative to the C-O-C peak and both decreased in size relative to the amide III in the thermal experiments. From Figure 6, however, it appears that regions with higher TEG content tend to also have a lower C-O-H to C-O-C absorbance ratio. If the difference in thermal response seen were because of different absorbance sensitivities to concentration in the two different functional groups the opposite would be seen. This supports the hypothesis that some of the OH groups in TEG are interacting with other species and this seems to be more prominent in TEG-rich phases in the processed material.

Table IV. Summary Statistics for Grids Mapped on Consolidated Plastics

	TEG/amide III			C-O-H/C-O-C		
	ENTP	INTP	CNTP	ENTP	INTP	CNTP
Mean	1.56	1.37	1.59	1.88	1.76	1.71
Standard deviation	0.08	0.14	0.11	0.07	0.09	0.13
Lower quartile	1.50	1.25	1.51	1.83	1.71	1.63
Median	1.56	1.37	1.60	1.87	1.75	1.70
Upper quartile	1.61	1.51	1.67	1.93	1.80	1.77

Filtered for a minimum integrated area of 1 under the amide III region to exclude points outside microtomed ribbons.

It is interesting to note that the average TEG to amide III ratio in the processed materials (Table IV) is above that of the pre-extruded material after even a 2-min heat treatment (Table II), and well above that of the more slowly treated material tested at incremental temperatures (Table III). This would suggest that even if TEG is being driven off during thermal experiments for FT-IR, it is not significantly removed by processing. The overall reduction in peak intensity, relative to the amide III region could initially suggest that TEG is being driven off by evaporation. This, however, was thought to be unlikely as the boiling point of TEG is around 288°C. The boiling point of TEG water mixtures does drop below this, down to 125°C with 10% water to below 120°C with greater than 20% water.[25] However, in such mixtures it would typically be the more volatile species that would evaporate off first.

TGA

Constant Rate. To confirm whether or not mass loss attributable to evaporation of TEG was occurring at the temperatures tested in the FT-IR thermal analysis, samples were examined by TGA. Samples of freeze dried-PNTP showed very little mass loss below 120°C. The small amount that did occur would be better attributed to the last amount of moisture being removed. The larger mass loss event occurring between 150°C and 250°C could correspond to TEG evaporating. This mass loss was associated with an endothermic event, consistent with volatilization (Figure 7). Furthermore, the event was not seen in bloodmeal alone or in FD-PNTP-V0 (without TEG), though some mass loss occurred in FD PNTP-V0 at the higher end of this range (Figure 8). This demonstrated that TEG evaporated from the material above 150°C, not below 120°C, in a typical TGA experiment.

It should be noted that the typical sample mass used in the TGA experiments of 10 mg is considerably larger than the individual particles tested in the synchrotron FT-IR experiments. Furthermore, the sample holder is a small crucible, and the typical sample ends up in a layer about 1–2 mm thick in the bottom of this. In the spatial maps of TEG distribution discussed above, migration of TEG into rich and poor zones in single particles was seen after even a brief heat treatment (Figure 4), indicating some amount of diffusion through the particle. The surface area to volume ratio for a single particle on a barium

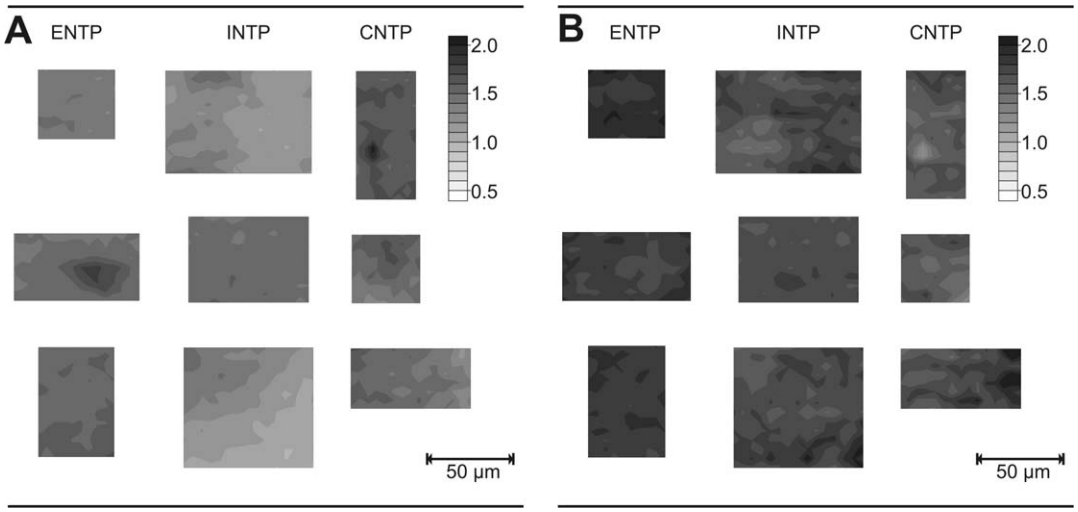

Figure 6. Spatial maps for microtomed sections of bloodmeal-based plastics after extrusion, injection moulding and conditioning. (A) Ratio between peak integrals representing TEG (1040–1150 cm^{-1}) and the amide III region (1180–1330 cm^{-1}); darker shading indicates higher relative TEG content. (B) Ratio between peak integrals representing C-O-H bonds in TEG (1040–1095 cm^{-1}) and C-O-C bonds in TEG (1095–1150 cm^{-1}); darker shading indicates larger relative C-O-H absorbance. Three separate grids are shown for each processing step.

fluoride slide is much greater than for what is effectively a packed column (albeit a small one in TGA). The sample size is deliberately kept small to minimize the effect of diffusion rates on mass loss temperatures, but TEG has been shown to have a strong interaction with proteins which may slow the diffusion rate to where it is significant in TGA.

Isothermal. Isothermal (120°C) TGA experiments on PNTP-V0 and PNTP-TEG found a mass loss greater than the amount of water added to the formulation (Table V). A small mass loss would be expected, as the moisture content of bloodmeal itself is approximately 5 wt % (determined from TGA of bloodmeal alone), corresponding to about 4 wt % of the blended NTP formulation. For PNTP, the amount corresponds to bound water in bloodmeal used in the formulation, but for PNTP-TEG, this additional mass loss exceeds that. It was thought that this may be the result of urea degradation, as TEG was more tightly bound to the protein. However, with no urea present, a similar mass loss was seen (Table V). In all three formulations, the mass loss to 100°C corresponded with the mass of water added in the sample. Only 0–1% of the total starting mass came off between 100°C and 120°C, but both of the formulations with TEG had the extra mass loss, whether urea was included or not. This would then confirm that TEG can be volatilized given enough time.

TEG volatilization during thermoplastic processing is not a great concern as the residence time in the extruder and injection moulder at 120°C is short relative to the experimental times reported in Table V. Nevertheless, it does suggest that as increased folding into β-sheets occurs, TEG is displaced and will migrate out of particles over time at elevated temperatures.

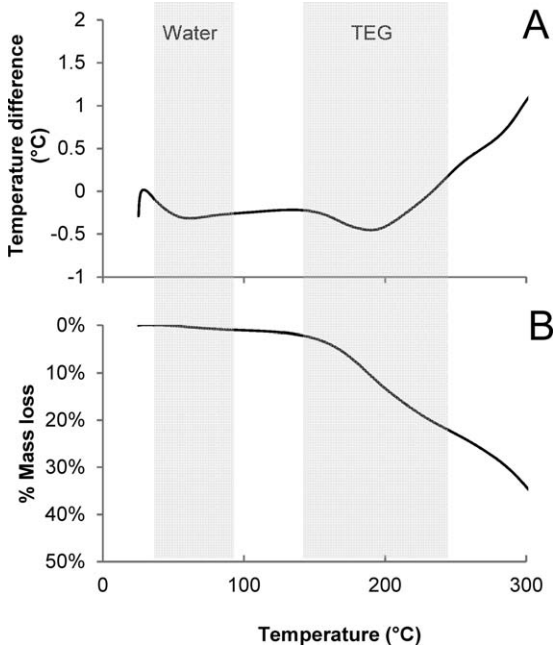

Figure 7. TGA thermograms of (A) temperature difference, and (B) mass loss for FD PNTP-TEG.

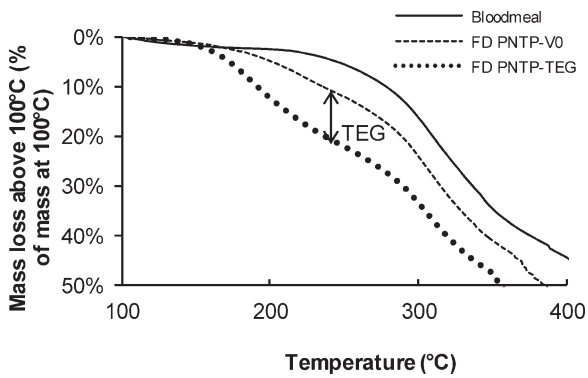

Figure 8. TGA thermograms of mass loss between 100°C and 400°C for bloodmeal, and FD PNTP with and without TEG.

Table V. Percentage Plasticizer and Mass Loss During Isothermal TGA Experiments

		PNTP-TEG (%)	PNTP-V0 (%)	PNTP-U0 (%)
Percentage plasticisers (wet basis)	Added water	23	34	24
	Assumed water in bloodmeal	4	4	4
	Total water	27	38	28
	Percentage urea	9	9	0
	Percentage TEG	11	0	12
Percentage mass loss during heating to	100°C	23	34	24
	120°C	23	35	25
Percentage mass loss during heating to 120°C followed by isothermal hold time of	60 min	30	36	30
	120 min	31	37	32
	180 min	32	37	32
Difference between mass loss at 3 h and added water (% of total starting mass)		9	3	8

The glass transition (T_g) of freeze dried PNTP-V0, determined by DMA in a material pocket is approximately 154°C in contrast to 64°C for freeze dried PNTP-TEG.[20] After removing water, material without TEG is below its T_g at 120°C, whereas material with TEG is still above its T_g. Immobilized, tightly packed protein chains have barrier properties that will restrict the passing of small molecules. With TEG, conformational mobility at 120°C will still allow both the motion of TEG and of other small molecules in the material, enabling both TEG and any degradation products to diffuse out over time.

CONCLUSIONS

TEG present in NTP accumulates in discrete areas then migrates towards the periphery and evaporates upon heating. These happen in parallel to an increase in β-sheet structures. Given TEG bonding to NTP and β-sheet formation involve hydrogen bonding, it suggests that on heating, β-sheet formation is favored, pushing TEG out of NTP. This plasticizer migration and evaporation occurs very slowly, therefore NTP is largely unaffected by it during the thermal processes in extrusion and injection moulding. However, it does mean that NTP should not be exposed to high temperatures for prolonged periods.

ACKNOWLEDGMENTS

This research was undertaken on the infrared microspectroscopy beamline at the Australian Synchrotron, Victoria, Australia. Proposal numbers AS113/IRMFI/4267 and AS122/IRMFI/4951 and The authors would especially like to acknowledge the technical assistance of Dr. Mark Tobin and Dr Danielle Martin. Travel funding support was received from the New Zealand Synchrotron Group Ltd.

REFERENCES

1. Verbeek, C. J. R.; Viljoen, C.; Pickering, K. L.; van den Berg, L. E. Plastic Material. NZ Patent NZ551531, **2007**.
2. Verbeek, C. J. R.; van den Berg, L. E. *J. Polym. Environ. 1*, **2010**.
3. Verbeek, C. J. R.; van den Berg, L. E. *Macromol. Mater. Eng.* **2010**, *295*, 10.
4. Verbeek, C. J. R.; van den Berg, L. E. *Macromol. Mater. Eng.* **2011**, *296*, 524.
5. Bier, J.; Verbeek, C. J. R.; Lay, M. C. *Macromol. Mater. Eng. 10*.1002/mame.2012004602013.
6. Pommet, M.; Redl, A.; Guilbert, S.; Morel, M. -H. *J. Cereal Sci.* **2005**, *42*, 81.
7. Mo, X.; Sun, X. *J. Polym. Environ.* **2003**, *11*, 15.
8. di Gioia, L.; Guilbert, S. *J. Agric. Food Chem.* **1999**, *47*, 1254.
9. Rahman, M.; Brazel, C. S. *Prog. Polym. Sci.* **2004**, *29*, 1223.
10. Petersen, J. H.; Breindahl, T. *Food Addit. Contam.* **2000**, *17*, 133.
11. Vieira, M. G. A.; da Silva, M. A.; dos Santos, L. O.; Beppu, M. M. *Eur. Polym. J.* **2011**, *47*, 254.
12. Orliac, O.; Rouilly, A.; Silvestre, F.; Rigal, L. *Ind. Crops Prod.* **2003**, *18*, 91.
13. Chen, P.; Zhang, L. *Macromol. Biosci.* **2005**, *5*, 237.
14. Kunanopparat, T.; Menut, P.; Morel, M. H.; Guilbert, S. *Compos. Part A: Appl. Sci. Manuf.* **2008**, *39*, 777.
15. Olabarrieta, I.; Cho, S. W.; Gallstedt, M.; Sarasu, J. R.; Johansson, E.; Hedenqvist, M. S. *Biomacromolecules* **2006**, *7*, 1657.
16. Wan, V. C. H.; Kim, M. S.; Lee, S. Y. *J. Food Sci.* **2005**, *70*, E387.
17. Thomazine, M.; Carvalho, R. A.; Sobral, P. I. A. *J. Food Sci.* **2005**, *70*, E172.
18. Guerrero, P.; Retegi, A.; Gabilondo, N.; de la Caba, K. *J. Food Eng.* **2010**, *100*, 145.
19. Chen, P.; Tian, H.; Zhang, L.; Chang, P. R. *Ind. Eng. Chem. Res.* **2008**, *47*, 9389.

20. Bier, J. M.; Verbeek, C. J. R.; Lay, M. C. *J. Appl. Polym. Sci.* **2013**, *130*, 359.
21. Yu, P. Q.; McKinnon, J. J.; Christensen, C. R.; Christensen, D. A. *J. Agric. Food Chem.* **2004**, *52*, 7353.
22. Selling, G. W. *Polym. Degrad. Stabil.* **2010**, *95*, 2241.
23. Barone, J. R.; Arikan, O. *Polym. Degrad. Stabil.* **2007**, *92*, 859.
24. Tian, K.; Porter, D.; Yao, J.; Shao, Z.; Chen, X. *Polymer* **2010**, *51*, 2410.
25. Dow Chemical Company. **2007**.